

RSC Advances



This is an *Accepted Manuscript*, which has been through the Royal Society of Chemistry peer review process and has been accepted for publication.

Accepted Manuscripts are published online shortly after acceptance, before technical editing, formatting and proof reading. Using this free service, authors can make their results available to the community, in citable form, before we publish the edited article. This *Accepted Manuscript* will be replaced by the edited, formatted and paginated article as soon as this is available.

You can find more information about *Accepted Manuscripts* in the [Information for Authors](#).

Please note that technical editing may introduce minor changes to the text and/or graphics, which may alter content. The journal's standard [Terms & Conditions](#) and the [Ethical guidelines](#) still apply. In no event shall the Royal Society of Chemistry be held responsible for any errors or omissions in this *Accepted Manuscript* or any consequences arising from the use of any information it contains.

Cite this: DOI: 10.1039/c0xx00000x

www.rsc.org/xxxxxx

COMMUNICATIONS

One-step synthesis of aluminum magnesium oxide nanocomposites for simultaneous removal of arsenic and lead ions in waterFeng Xiao,^{*a} Liping Fang,^{a,b} Wentao Li^a and Dongsheng Wang^a

Received (in XXX, XXX) Xth XXXXXXXXXX 20XX, Accepted Xth XXXXXXXXXX 20XX

DOI: 10.1039/b000000x

Aluminum magnesium oxide nanocomposites are prepared via a one-step microwave assisted solvothermal method, and they show high adsorption capacities for removal both of As (V) and Pb (II) ions in water.

Heavy metal ions, such as As (V), Pb (II) and Cd (II), are highly toxic pollutants, which can have serious side effects and toxicities on human health when their concentrations are higher than permissible limits.¹⁻³ Therefore, their efficient removal from water is an actively pursued goal in these years. Various methods, including chemical coagulation, ion exchange, membrane process, electrochemical method, and adsorption, have been developed for the removal of these heavy metal ions.³⁻¹⁵ Among these methods, adsorption technique is perhaps the most extensively adopted due to its low cost and simplicity. However, traditional adsorbents such as activated carbon, activated alumina, clay and zeolite show limited adsorption abilities for heavy metal ions. Nanomaterials, including metal oxides with hierarchical nanostructures and layered double hydroxides, have shown excellent adsorption capacities for heavy metal ions removal.¹⁴⁻²⁰ The adsorption capacity of nanomaterials can be attributed to high surface area, facile mass transportation and abundance active adsorption sites. Song *et al.* developed many different kinds of nanomaterials, such as flowerlike α -Fe₂O₃, CeO₂ hollow nanospheres, ordered mesoporous γ -Al₂O₃, urchin zinc silicate, which showed higher adsorption capacities than commercial adsorbents.²¹⁻²⁸ Recently, they reported a novel protocol of synthesizing flowerlike magnesium oxides and aluminum basic carbonate microporous nanospheres for removal of Pb (II) and As (V) with maximum adsorption capacities of 1980 mg/g and 170 mg/g, respectively.^{29, 30} Despite these outstanding achievements having been obtained, most of the results can only removal either negatively charged heavy metal anions or positively charged heavy metal cations alone.

Wang *et al.* and Lou *et al.* fabricated chrysanthemum-like α -FeOOH³¹ and urchin-like α -FeOOH hollow nanospheres³², respectively, and found their good adsorption property for both of As (V) and Pb (II). Yang *et al.* prepared hierarchical porous magnetic nanomaterial with high adsorption capacities for removal of Pb (II), As (V) and Cr (VI) ions from aqueous solution.³³ However, the adsorption capacities of these adsorbents are still relatively low. In addition, expensive chemicals and complicated synthesis processes are usually used, which limit their practical applications. Therefore, there is an urgent demand

for developing a low-cost and facile method to fabricate nanomaterials with high adsorption capacities for removing various cationic and anionic heavy metal ions.

Herein, we present a facile one-step synthesis of aluminum magnesium oxide nanocomposites via microwave assisted solvothermal method, which is a simple, template-free and low-cost route. In addition, the morphologies and structures of obtained aluminum magnesium oxide nanocomposites can be easily tuned through changing the molar ratio of Al³⁺ and Mg²⁺ addition. These nanocomposites had large surface area and showed excellent adsorption properties for both As (V) and Pb (II) with maximum adsorption capacities of 133 mg/g and 423 mg/g, respectively.

In a typical synthesis, certain amount of Al(NO₃)₃•9H₂O, Mg(NO₃)₂•6H₂O (total metal molar is 10 mmol) and 20 mmol of urea were dissolved in 100 mL of anhydrous ethanol under sonication to form clear solution, and then about 40 mL solution was poured into a Teflon-lined autoclave for microwave heating. The oven was heated to 150 °C in 2 min by microwave irradiation, and then kept at that temperature for additional 30 min. Precipitates were collected by centrifugation after cooling to room temperature, and then washed with water and ethanol. Finally the samples were dried at 80 °C for 5 h. The detail experiment procedures are shown in the supplementary information. Samples obtained with different molar ratio of Al³⁺ and Mg²⁺ were defined as Al_xMg_y nanocomposites, x is the molar of Al(NO₃)₃•9H₂O and y is the molar of Mg(NO₃)₂•6H₂O.

Unlike previously reported methods with multistep for synthesis of nanocomposites,³³ one-step microwave assisted solvothermal method without organic template or solvent is used to prepare hierarchical aluminum magnesium oxide nanocomposites in this work. Microwave heating has major advantages in cost- and time-efficient, with which the reaction time for the solvothermal process can be fulfilled within 30 min. In addition, microwave heating leads to uniform heating of the whole synthesis mixture, resulting in homogeneous nanocomposites in shape and size. Overall, this method is facile, low-cost and environment-friendly.

Fig. 1a shows the typical SEM image of Al₃Mg₇ nanocomposites samples, where the surface of the nanocomposites was rough and many sheets were deposited on the surface. TEM images (Fig. 1b) clearly shows that Al₃Mg₇ nanocomposites are composed of "graphene-like" sheets wrapped with nanospheres. The corresponding X-ray diffraction (XRD)

pattern for the Al_3Mg_7 nanocomposites is shown in Fig. 1c. All diffraction peaks can be indexed to $\text{Mg}_2(\text{OH})_{3.24}(\text{NO}_3)_{0.76}(\text{H}_2\text{O})_{0.24}$ (JCPDS 47-0436), while no obvious diffraction peaks of aluminum chemicals were observed, suggesting aluminum chemicals may exist as amorphous form. The Energy dispersive spectrum (EDS) (Fig. S1, ESI†) indicated that the sample consisted of carbon, oxygen, aluminum and magnesium.

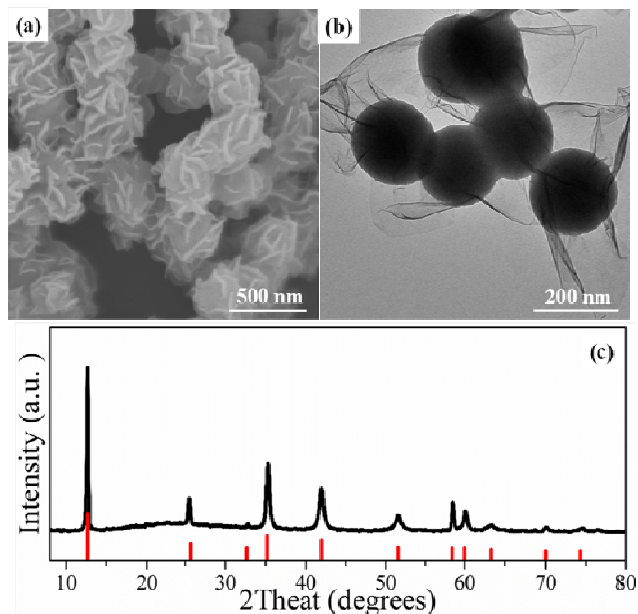


Fig. 1 (a) SEM image, (b) TEM image and (c) XRD pattern of typical sample of Al_3Mg_7 nanocomposites.

In order to investigate the formation process and the structures of Al_3Mg_7 nanocomposites, samples prepared at different reaction times are collected and investigated by SEM, XRD and EDS. Solid and amorphous spheres with average diameters of ca. 200 nm are obtained in 5 min (Fig. S2). More interestingly, neither of magnesium nor nitrogen was detected in the EDS spectrum, indicating there was no magnesium containing chemicals formed during this reaction time, meanwhile, the XRD pattern also showed no diffraction peak. When the reaction time was prolonged to 30 min, “graphene-like” sheets wrapped with nanospheres were observed, and magnesium chemicals were also formed, as discussed above. It is worth to mention that the diameter of inner nanospheres was nearly the same as those obtained in 5 min, suggesting that magnesium chemicals were formed after 5 min and wrapped the surface of inner nanospheres. During 5 min, the synthesis procedures in this communication were similar to the previous paper reported by Song *et al.*, where the samples were defined as $\text{Al}(\text{OH})\text{CO}_3$ nanospheres.³⁰ Therefore, we can ascribe the solid and amorphous inner nanospheres formed during 5 min as $\text{Al}(\text{OH})\text{CO}_3$. After 5 min, “graphene-like” sheets of $\text{Mg}_2(\text{OH})_{3.24}(\text{NO}_3)_{0.76}(\text{H}_2\text{O})_{0.24}$ grew and wrapped $\text{Al}(\text{OH})\text{CO}_3$ nanospheres to form the final aluminum magnesium oxide nanocomposites. The possible reason for forming these structures was the different nucleation speed of $\text{Al}(\text{OH})\text{CO}_3$ and $\text{Mg}_2(\text{OH})_{3.24}(\text{NO}_3)_{0.76}(\text{H}_2\text{O})_{0.24}$.

In addition, the morphologies and structures of aluminum magnesium oxide nanocomposites can be easily tuned through

changing the molar ratio of Al^{3+} and Mg^{2+} . As shown in Fig. 2, aluminum magnesium oxide nanocomposites with different sizes of “graphene-like” sheets and inner nanospheres were obtained. With increasing Mg^{2+} concentration or decreasing Al^{3+} concentration, the size of “graphene-like” sheets became bigger and the inner $\text{Al}(\text{OH})\text{CO}_3$ nanospheres became smaller.

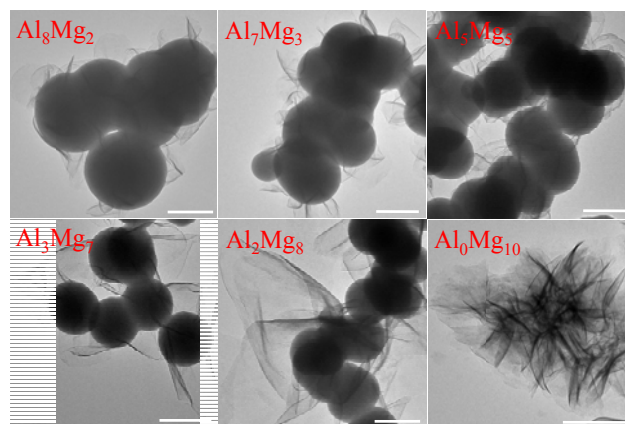


Fig. 2 TEM images of aluminum magnesium oxide nanocomposites with different molar ratio of aluminum and magnesium. (Scale bars: 200 nm)

Nitrogen adsorption-desorption isotherms of aluminum magnesium oxide nanocomposites with different molar ratio of aluminum and magnesium were shown in Fig. 3. The Brunauer-Emmett-Teller (BET) surface area of Al_8Mg_2 , Al_7Mg_3 , Al_5Mg_5 , Al_3Mg_7 and Al_2Mg_8 nanocomposites were 270, 262, 220, 191 and 126 m^2/g , respectively. The gradual decrease of specific surface area with the decrease of aluminum contents was due to that the inner $\text{Al}(\text{OH})\text{CO}_3$ nanospheres were microporous structures and had higher specific surface area. These aluminum magnesium oxide nanocomposites with different chemical structures and surface areas have different adsorption properties for heavy metal ions.

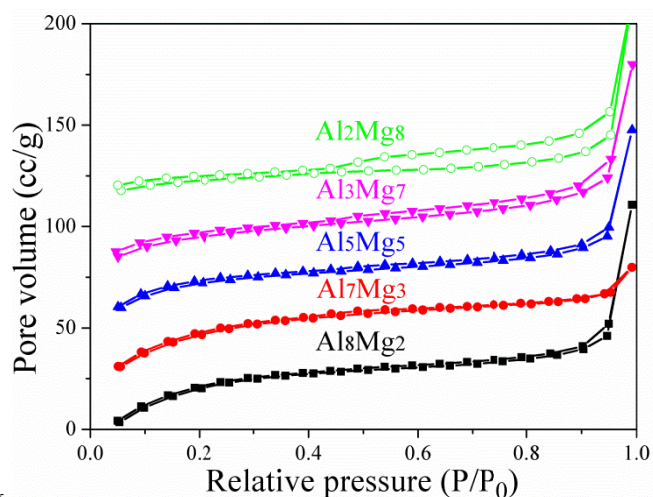


Fig. 3 Nitrogen adsorption-desorption isotherms of aluminum magnesium oxide nanocomposites with different molar ratio of aluminum and magnesium.

Due to the high specific surface area of the aluminum magnesium oxide nanocomposites, they were expected to show advantage in heavy metal ions adsorption. As (V) and Pb (II) are

two typical toxic heavy metal ions in water resources, and their efficient removal is of great importance. Fig. S3 shows the adsorption rates of As (V) and Pb (II) solutions with an initial concentration of 50 mg L⁻¹ on the Al₈Mg₂ spheres at room temperature. The adsorption processes are very fast as the equilibriums are reached in only 30 min. Fig. 4a and Fig. 4b show the adsorption isotherms of aluminum magnesium oxide nanocomposites with different molar ratio of aluminum and magnesium for As (V) and Pb (II), respectively. The adsorption data were fitted with the Langmuir model as follows:

$$q_e = q_m b C_e / (1 + b C_e)$$

Where C_e is the equilibrium concentration of heavy metal ions (mg/L), q_e is the amount of heavy metal ions adsorbed per unit weight of the adsorbent at equilibrium (mg/g), q_m (mg/g) is the maximum adsorption capacity and b is the equilibrium constant related to the adsorption energy.

It showed that the experimental data agreed well with Langmuir model, indicating the mono-surface complexation processes. The maximum adsorption capacities of aluminum magnesium oxide nanocomposites can be calculated according to the fitting curves, as shown in Fig. 4c. The maximum adsorption capacities for As (V) and Pb (II) were 133 mg/g on Al₈Mg₂ and 423 mg/g on Al₂Mg₈, respectively. These values are significantly higher than the values in recent literatures that can both adsorb anions and cations, as shown in Table 1. In addition, these adsorbents can be regenerated with NaOH (0.1 M) for re-usability. Taking Al₈Mg₂ spheres for example, a recycling test shows that their capacities can be maintained as 124 mg/g and 200 mg/g for As (V) and Pb (II) after regeneration.

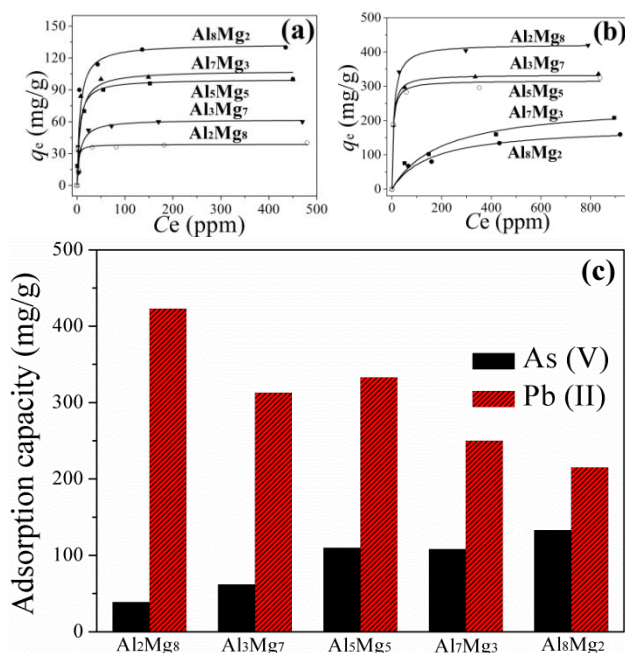


Fig. 4 Adsorption isotherms of (a) As (V), (b) Pb (II) and (c) maximum adsorption capacities on aluminum magnesium oxide nanocomposites with different molar ratio of aluminum and magnesium.

Table 1. Maximum adsorption capacities of different adsorbents for As (V) and Pb (II)

Adsorbents	Maximum adsorption capacity (mg/g)	
	As (V)	Pb (II)
Al ₈ Mg ₂ (this study)	133	215
Al ₂ Mg ₈ (this study)	38.7	423
Chrysanthemum-like α -FeOOH ³¹	66.2	103
Urchin-like α -FeOOH hollow nanospheres ³²	58	80
Porous magnetic Fe ₂ O ₃ @AlO(OH) ³³	74.9	84.1

Difference of adsorption capacities for Pb (II) and As (V) on the aluminum magnesium oxide nanocomposites with different molar ratio of Al³⁺ and Mg²⁺ can be ascribed to the following reasons. According to the literatures, the active adsorption sites for As (V) and Pb (II) are aluminum and magnesium, respectively.^{29, 30} Therefore, when amount of aluminum in the composite is high, adsorption capacity for As (V) is also high, while adsorption capacity for Pb (II) is low. On the contrary, low adsorption capacity for As (V) and high adsorption capacity for Pb (II) can be found when low aluminum and high magnesium are in the composites. Moreover, aluminum magnesium oxide nanocomposites with different chemical structures showed different surface areas, which also affected the adsorption properties for heavy metal ions.

In conclusion, aluminum magnesium oxide nanocomposites were prepared via one-step microwave assisted solvothermal method. This is a simple, template-free and low-cost route. These nanocomposites had large surface area and could adsorb both heavy metal anions and cations. The maximum adsorption capacities for As (V) and Pb (II) were 133 mg/g and 423 mg/g, respectively.

Acknowledgements

We gratefully thank the National Basic Research Program from Ministry of Science and Technology (no.2011CB933700), National Natural Science Foundation of China (no. 51378014, 51338008, 51338010).

Notes and references

- ^a Key Laboratory of Drinking Water Science and Technology, Research Center for Eco-Environmental Sciences, Chinese Academy of Sciences, No.18, Shuangqing Road, Haidian District, Beijing, 100085, China. Fax: +86 10 6284 9138; Tel: +86 10 62849 138; E-mail: fengxiao@rcees.ac.cn
- ^b Faculty of Material Science and Chemistry, China University of Geosciences, No.388, Lumo Road, Wuhan, 430074, China.
- † Electronic Supplementary Information (ESI) available: [EDS spectra of aluminum magnesium oxide nanocomposites obtained at 5 min and 30 min]. See DOI: 10.1039/b000000x/

- R. P. Schwarzenbach; B. I. Escher; K. Fenner; T. B. Hofstetter; C. A. Johnson; U. von Gunten; B. Wehrli, *Science* **2006**, *313*, 1072.
- C. T. Yavuz; J. T. Mayo; W. W. Yu; A. Prakash; J. C. Falkner; S. Yean; L. Cong; H. J. Shipley; A. Kan; M. Tomson; D. Natelson; V. L. Colvin, *Science* **2006**, *314*, 964.
- I. Ali, *Chem. Rev.* **2012**, *112*, 5073.

4. L. Charentanyarak, *Water Science and Technology* **1999**, *39*, 135.
5. A. M. Shahalam; A. Al-Harthy; A. Al-Zawhry, *Desalination* **2002**, *150*, 235.
6. S. Babel; T. A. Kurniawan, *J. Hazard. Mater.* **2003**, *97*, 219.
- 5 7. K. Vaaramaa; J. Lehto, *Desalination* **2003**, *155*, 157.
8. P. Cañizares; F. Martínez; C. Jiménez; J. Lobato; M. A. Rodrigo, *Environ. Sci. Technol.* **2006**, *40*, 6418.
9. N. P. Hankins; N. Lu; N. Hilal, *Separation and Purification Technology* **2006**, *51*, 48.
- 10 10. J. L. Huisman; G. Schouten; C. Schultz, *Hydrometallurgy* **2006**, *83*, 106.
11. K. Trivunac; S. Stevanovic, *Chemosphere* **2006**, *64*, 486.
12. D. Mohan; C. U. Pittman Jr, *J. Hazard. Mater.* **2007**, *142*, 1.
13. A. G. El Samrani; B. S. Lartiges; F. Villiérás, *Water Res.* **2008**, *42*,
15 951.
14. J. S. Hu; L. S. Zhong; W. G. Song; L. J. Wan, *Adv. Mater.* **2008**, *20*, 2977.
15. D. Chen; L. Cao; T. L. Hanley; R. A. Caruso, *Adv. Funct. Mater.* **2012**, *22*, 1966.
- 20 16. M. M. Tong; X. D. Zhao; L. T. Xie; D. H. Liu; Q. Y. Yang; C. L. Zhong, *Progress in Chemistry* **2012**, *24*, 1646.
17. J. W. Liu; H. W. Liang; S. H. Yu, *Chem. Rev.* **2012**, *112*, 4770.
18. M. Hua; S. Zhang; B. Pan; W. Zhang; L. Lv; Q. Zhang, *J. Hazard. Mater.* **2012**, *211–212*, 317.
- 25 19. Z. X. Wu; D. Y. Zhao, *Chem. Commun.* **2011**, *47*, 3332.
20. H. W. Liang; X. Cao; W. J. Zhang; H. T. Lin; F. Zhou; L. F. Chen; S. H. Yu, *Adv. Funct. Mater.* **2011**, *21*, 3851.
21. Qu, J.; C. Y. Cao; Y. L. Hong; C. Q. Chen; P. P. Zhu; W. G. Song; Z. Y. Wu, *J. Mater. Chem.* **2012**, *22*, 3562.
- 60 22. C. Y. Cao; J. Qu; W. S. Yan; J. F. Zhu; Z. Y. Wu; W. G. Song, *Langmuir* **2012**, *28*, 4573.
23. W. Li; C.-Y. Cao; L.-Y. Wu; M.-F. Ge; W.-G. Song, *J. Hazard. Mater.* **2011**, *198*, 143.
- 65 24. C. Y. Cao; Z. M. Cui; C. Q. Chen; W. G. Song; W. Cai, *J. Phys. Chem. C* **2010**, *114*, 9865.
25. L. S. Zhong; J. S. Hu; A. M. Cao; Q. Liu; W. G. Song; L. J. Wan, *Chem. Mater.* **2007**, *19*, 1648.
26. L. S. Zhong; J. S. Hu; H. P. Liang; A. M. Cao; W. G. Song; L. J. Wan, *Adv. Mater.* **2006**, *18*, 2426.
- 70 27. C.-Y. Cao; F. Wei; J. Qu; W.-G. Song, *Chem. Eur. J.* **2013**, *19*, 1558.
28. J. Qu; W. Li; C.-Y. Cao; X.-J. Yin; L. Zhao; J. Bai; Z. Qin; W.-G. Song, *J. Mater. Chem.* **2012**, *22*, 17222.
29. C.-Y. Cao; J. Qu; F. Wei; H. Liu; W.-G. Song, *ACS Appl. Mater. Interfaces* **2012**, *4*, 4283.
- 75 30. C.-Y. Cao; P. Li; J. Qu; Z.-F. Dou; W.-S. Yan; J.-F. Zhu; Z.-Y. Wu; W.-G. Song, *J. Mater. Chem.* **2012**, *22*, 19898.
31. H. Li; W. Li; Y. J. Zhang; T. S. Wang; B. Wang; W. Xu; L. Jiang; W. G. Song; C. Y. Shu; C. R. Wang, *J. Mater. Chem.* **2011**, *21*, 7878.
- 80 32. B. Wang; H. Wu; L. Yu; R. Xu; T.-T. Lim; X. W. Lou, *Adv. Mater.* **2012**, *24*, 1111.
33. X. Yang; X. Wang; Y. Feng; G. Zhang; T. Wang; W. Song; C. Shu; L. Jiang; C. Wang, *J. Mater. Chem. A* **2013**, *1*, 473.

85

30

35

40

45

50

55